Design and Realization of CPW Circuits Using EC-ANN Models for CPW Discontinuities *

Hu Jiang[1] and Sun Lingling[2]

(1 Department of Information Science & Electronic Engineering, Zhejiang University, Hangzhou 310027, China)
(2 Microelectronic CAD Center, Hangzhou Dianzi University, Hangzhou 310018, China)

Abstract: Novel accurate and efficient equivalent circuit trained artificial neural-network (EC-ANN) models, which inherit and improve upon EC model and EM-ANN models' advantages, are developed for coplanar waveguide (CPW) discontinuities. Modeled discontinuities include: CPW step, interdigital capacitor, symmetric cross junction, and spiral inductor, for which validation tests are performed. These models allow for circuit design, simulation, and optimization within a CAD simulator. Design and realization of a coplanar lumped element band pass filter on GaAs using the developed CPW EC-ANN models are demonstrated.

Key words: CPW; discontinuities; models; equivalent circuit; artificial neural-network; band pass filter
EEACC: 2570A
CLC number: TN43 **Document code:** A **Article ID:** 0253-4177(2005)12-2320-10

1 Introduction

Coplanar waveguide (CPW) circuits are widely used in microwave integrated circuits (MICs) as well as monolithic microwave integrated circuits (MMICs) because of their many advantages due to the CPW configuration, such as the ease of shunt and series connections, low radiation, low dispersion, and simplification of fabrication[1]. Current, design software available for CPW circuits is inadequate because of the nonavailability of accurate and efficient models for CPW discontinuities, including open, gap, step, cross-junction, and spiral-inductor. Accurate characterization and modeling of these components are vital for accurate circuit simulation and an increased first-pass design success rate.

Much effort has been expended in analyzing and modeling CPW discontinuities. Equivalent circuit (EC) models with different numerical electromagnetic (EM) simulation methods are the most universal models[2~7]. EC models can characterize their CPW components in a wide band, and can be conveniently used in circuit simulation and optimization. However, the time-consuming nature of EM simulation limits their use for interactive CAD and circuit optimization. The two other EC models are based on analytical methods[8,9], which are not available for most CPW discontinuities now, and empirical formulae[10,11], whose range and accuracy are limited. Recently, artificial neural networks (ANN) have been applied to CPW discontinuity modeling, which can be trained to learn any arbitrary nonlinear input-output relationship from corresponding data to provide a fast result to the task they have learned. Neural networks are efficient alternatives to conventional methods such as numerical modeling methods, analytical methods, and empirical models. Electromagnetically trained artificial neural-network (EM-ANN) models employ full-wave EM simulation data to characterize the CPW components[13,14]. Despite ANN's inherent advantages, it is time-consuming to obtain enough input parameters (geometry parameter, frequency param-

* Project supported by the National Natural Science Foundation of China (No. 90207007) and the Key Cooperation Plan of Zhejiang Province (No. 2004C14004)
Received 9 July 2005

eter ,etc.) and output parameters (*S*-parameters) for insuring the model 's accuracy in a wide band , and it is less flexible than EC models in circuit simulation.

As a synthesis and improvement to the above , we have developed equivalent circuit trained artificial neural-network (EC-ANN) models for CPW discontinuities ,suitable for use in interactive (M) MICs design and optimization. First ,full-wave EM simulation is employed to characterize the CPW discontinuities for which the reference planes are placed at the physical discontinuity ones. Second , the wide band equivalent circuit parameters need to be extracted by certain arithmetic from *S*-parameters. Finally ,we use these data from the CPW discontinuities with different geometry parameters to train an ANN model. EC-ANN models have been developed for CPW steps , interdigital capacitors , symmetric cross junctions ,and spiral inductors in this paper. All models have been developed using Agilent ADS-Momentum for EM simulation. The cross-section of a back-grounded CPW is shown in Fig. 1. Common parameters for all models are the substrate parameters (ε_r = 12.9 , H_{sub} = h_1 = 100μm ,tanσ= 0.0016 , t = 3.5μm , back-grounded) . The frequency range of these models is about 0～40 GHz.

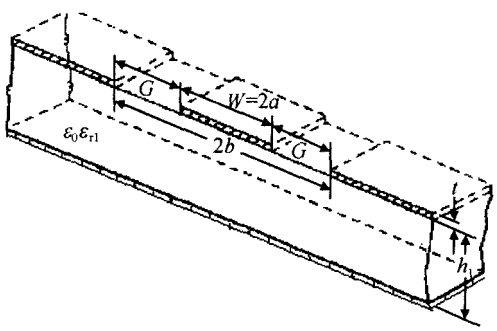

Fig. 1　Schematic of conductor backed CPW

Once developed , these EC-ANN models are linked to a commercial microwave-circuit simulator where they provide accuracy approaching that of the EM simulation tool used for characterization of the CPW components over the full ranges of the model input variables.

Circuit design using the developed EC-ANN CPW models is realized by a coplanar lumped element band pass filter. Simulation responses have been performed and compared to measured results of the entire circuit ,showing good agreement.

2　EC-ANN modeling

The methodology used for developing accurate and efficient EC-ANN models has some similarities to that for EM-ANN models , which has been detailed in several papers[12～15] . The ANN structure used in this paper is shown in Fig. 2 and consists of an input layer (X_n) , an output layer (Y_n) , and a hidden layer (W_{mn}) . It is a multilayer feed-forward ANN , utilizing the error-backpropagation learning algorithm. The hidden layer , which incorporates a nonlinear activation function , allows modeling of complex input/output relationships between multiple inputs and outputs. Inputs are connected to hidden layers by one set of weights and hidden layers are connected to the output layer by another set of weights. Training of the EC-ANN model is accomplished by adjusting these weights to give the desired response.

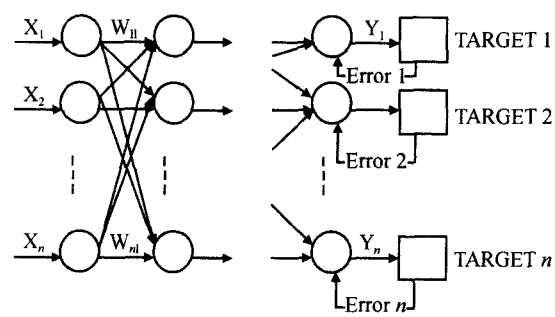

Fig. 2　A multilayer feed-forward ANN architecture

In the EC-ANN model ,the input data are geometry parameters of certain CPW discontinuities under consideration , and the output data are the corresponding wide band equivalent circuit parameters. First ,the input vectors of the training dataset are presented to the input neurons ,and the output vectors are computed. The ANN outputs are then compared to the known outputs (of the training

dataset) and the errors are computed. Error derivatives are then calculated and summed up for each weight until all the training examples have been presented to the network. These error derivatives are then used to update the weights for neurons in the model. Training proceeds until the errors are lower than prescribed values. There are three training algorithms (BP, Levenberg-Marquart, Quasinewton) and three activation functions (Sigmoid(), tanh(), Tansig()) used in ANN training in this paper. The best combination of training algorithm, activation function, and neuron number of hidden layer is chosen to reach the minimum training error. Details of the training algorithm are given in Refs. [16, 17].

In order to train EC-ANN models, a number of equivalent circuit parameters need to be extracted. These extracted equivalent circuit parameters represent important input/output relationships, which will be learned by EC-ANN models. They include a capacitive parameter (capacitance), an inductive parameter (inductance), and a losses parameter (resistor). For low metallic and dielectric losses, the losses parameter's influence on the equivalent circuit performance of CPW discontinuities in this paper is relatively low. Based on the "enough simplification to use" principle, the resistor is excluded from equivalent circuits in this paper. Because equivalent circuit parameters are frequency-independent, the frequency parameter is not included in the input data anymore. The training/test examples used in EC-ANN modeling are less than those in EM-ANN modeling, while covering more structures. Structures for EC-ANN modeling are chosen using the design of experiments (DOE) methodology[18], which can be used to determine simulation points which effectively cover the region of interest. When building a model, it helps to perform as few EM simulations as possible to achieve the desired accuracy.

3 EC-ANN model for CPW step

A step change in the width of the center strip conductor of a CPW and its equivalent circuit are shown in Fig. 3. The step discontinuity perturbs the normal CPW electric and magnetic fields and gives rise to additional reactances. These additional reactances are assumed to be lumped and located at the plane of the strip discontinuity.

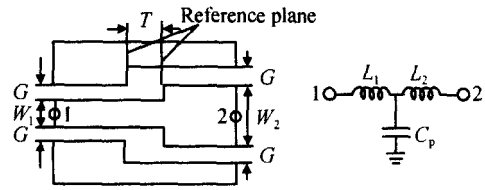

Fig. 3 CPW step and its equivalent-circuit

The step discontinuity has been modeled as a T-network consisting of two series inductances L_1 and L_2 and a shunt capacitance C_p, which can be extracted from the Z-parameter.

$$L_1 = \frac{\mathrm{Im}(Z_{11} - Z_{12})}{\omega} \tag{1}$$

$$L_2 = \frac{\mathrm{Im}(Z_{22} - Z_{21})}{\omega} \tag{2}$$

$$C = -\frac{1}{\omega \mathrm{Im}(Z_{12})} \tag{3}$$

According to electromagnetic theory, these equivalent circuit parameters are frequency independent. However, data calculated from momentum simulation results change by a very small amount with different frequencies, because of inherent error of the MoM (method of moments). Using the proper method can get the value with the best agreement between its momentum simulation and equivalent circuit simulation. Variable input parameters and corresponding ranges for model development are given in Table 1. Outputs of the model are L_1, L_2, and C_p. Momentum simulations have been performed on 196 structures (examples) over 0～40 GHz. The final data about ANN training are given in Table 2.

Table 1 Variable parameter ranges for CPW step

Parameter	Min	Max
W_1/μm	10	100
W_2/μm	10	100
G/μm	10	100
T/μm	10	30

Table 2　ANN training data of CPW step

Training algorithm	Levenberg-Marquardt
Activation function	Tansig()
Training error	4×10^{-6}
Neurone of the input layer	4
Neurone of the output layer	3
Neurone of the hidden layer	15

Finally, several structures are used to check the model's accuracy. They are not included in training examples, but in input parameters' ranges (similarly in the following section). To validate the capability of the model, some comparisons of the transmission coefficient $S(1,2)$ between momentum simulations and the obtained EC-ANN models simulations are presented in Fig. 4, and the agreement between the two results can be seen.

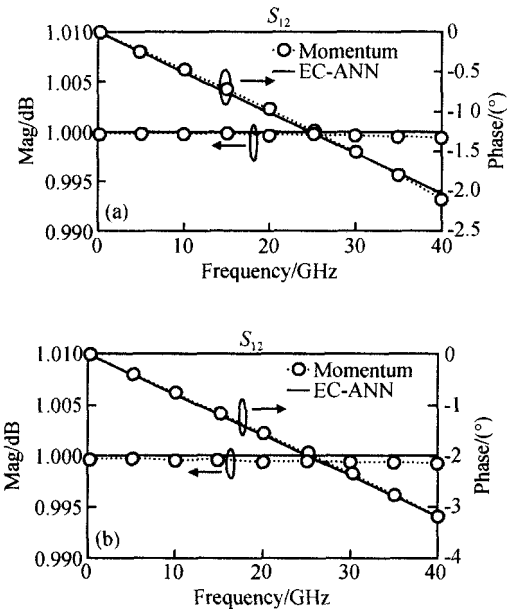

Fig. 4　Comparison EC-ANN for CPW step　(a) W_1 = 70μm, W_2 = 100μm, G = 10μm, T = 10μm; (b) W_1 = 50μm, W_2 = 80μm, G = 20μm, T = 20μm

4　EC-ANN model for CPW interdigital capacitor

In Fig. 5 the planform for a typical interdigital capacitor having seven fingers is shown. The interdigital capacitor for the purpose of circuit simulation can be represented by the π-equivalent circuit model shown in the inset in Fig. 5. In this model, the series capacitance C_s is the desired capacitance, while the shunt capacitance C_{p1} and C_{p2} are the parasitic capacitances between the interdigital structure and the CPW ground planes, whose extraction formulae are given in Eqs. (4)～(6).

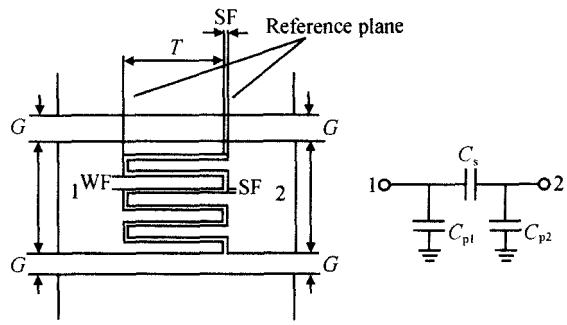

Fig. 5　CPW interdigital capacitor and its equivalent-circuit

$$C_{p1} = -\frac{1}{\omega \mathrm{Im}\left(\frac{Z_{11}Z_{22}-Z_{12}Z_{21}}{Z_{22}-Z_{21}}\right)} \tag{4}$$

$$C_{p2} = -\frac{1}{\omega \mathrm{Im}\left(\frac{Z_{11}Z_{22}-Z_{12}Z_{21}}{Z_{11}-Z_{12}}\right)} \tag{5}$$

$$C_s = -\frac{1}{\omega \mathrm{Im}\left(\frac{Z_{11}Z_{22}-Z_{12}Z_{21}}{Z_{12}}\right)} \tag{6}$$

The input parameters of the interdigital capacitor EC-ANN model include the interdigital finger type (N (N = 0 →WF = 5μm, SF = 5μm; N = 1 →WF = 10μm, SF = 5μm; N = 2 →WF = 15μm, SF = 5μm; N = 3 →WF = 20μm, SF = 5μm), half of the number of fingers n, CPW slot width G, and finger length T. Variable input parameters and the corresponding ranges for model development are given in Table 3. The output data of the model are C_{p1}, C_{p2}, and C_s. Momentum simulations have been performed on 240 structures (examples) over 0～40 GHz. Final ANN training data are given in Table 4.

Table 3　Variable parameter ranges for CPW interdigital capacitor

Parameter	Min	Max
N	0	3
n	1	5
G/μm	10	50
T/μm	20	120

Table 4 ANN training data of CPW interdigital capacitor

Training algorithm	BP
Activation function	Tansig()
Training error	2.5×10^{-5}
Neurone of the input layer	4
Neurone of the output layer	3
Neurone of the hidden layer	15

Some test examples are chosen to validate the model's availability in the input parameters' ranges. Because of its unsymmetrical two-port capacitive structure, some comparisons of return loss ($S(1,1)$, $S(2,2)$) and insertion loss $S(1,2)$ between momentum simulations and obtained EC-ANN model simulations are shown in Fig. 6. Except one or two high frequency points in Fig. 6(a), excellent agreement between the two results can be seen in the whole frequency range.

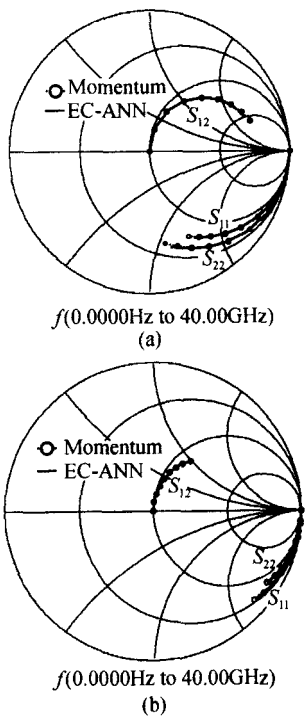

Fig. 6 Comparison EC-ANN for CPW interdigital capacitor (a) $N=1$ (WF = 10μm, SF = 5μm), $n=3.5$, $G=10$μm, $T=105$μm; (b) $N=1$ (WF = 10μm, SF = 5μm), $n=2.5$, $G=10$μm, $T=50$μm

5 EC-ANN model for CPW symmetric cross junction

The symmetric cross junction under consideration is shown on the left in Fig. 7. Since a cross junction includes several discontinuities, mode conversion takes place within the circuit. The excitation of the coupled slotline mode is suppressed by maintaining electrical continuity between the ground planes of the circuit. In this structure, the four CPW center strip conductors meet to form the junction while the continuity between ground planes at the junction is maintained by air-bridges.

A lumped element equivalent circuit model for the symmetric cross junction is shown on the right in Fig. 7. In this model, the inductances L_1 and L_s arise because of current flow interruptions. The capacitance C_p is the parasitic capacitance associated with the air-bridge. All these equivalent circuit parameters are extracted from Z-parameters.

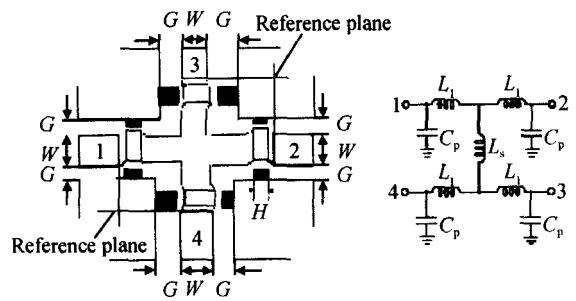

Fig. 7 CPW symmetric cross junction and its equivalent circuit

$$L_1 = \frac{\mathrm{Im}\left(\dfrac{Z_{11}Z_{31} - Z_{21}Z_{31} - Z_{11}Z_{21} + Z_{11}^2}{2Z_{31} + 2Z_{21}}\right)}{\omega} \tag{7}$$

$$L_s = \frac{\mathrm{Im}\left(\left(\dfrac{1}{Z_{11} - Z_{21}} - \left(\dfrac{Z_{11}Z_{31} - Z_{21}Z_{31} - Z_{11}Z_{21} + Z_{11}^2}{2Z_{31} + 2Z_{21}}\right)^{-1} + \dfrac{Z_{11}Z_{31} - Z_{21}Z_{31} - Z_{11}Z_{21} + Z_{11}^2}{2Z_{31} + 2Z_{21}}\right) \times \dfrac{Z_{21} - Z_{31}}{2Z_{31}}\right)}{\omega} \tag{8}$$

$$C_p = \frac{\mathrm{Im}\left(\dfrac{1}{Z_{11} - Z_{21}} - \left(\dfrac{Z_{11}Z_{31} - Z_{21}Z_{31} - Z_{11}Z_{21} + Z_{11}^2}{2Z_{31} + 2Z_{21}}\right)^{-1}\right)}{\omega} \tag{9}$$

The variable input parameters are W, G, and H, whose ranges are given in Table 5. Momentum simulations have been performed on 90 structures (examples) over 0～40 GHz. Final ANN training data are given in Table 6.

Table 5　Variable parameter ranges for CPW symmetric cross junction

Parameter	Min	Max
W/μm	10	100
G/μm	10	100
H/μm	20	60

Table 6　ANN training data of CPW symmetric cross junction

Training algorithm	Levenberg-Marquardt
Activation function	Tansig()
Training error	4.3×10^{-5}
Neurone of the input layer	3
Neurone of the output layer	3
Neurone of the hidden layer	15

Comparisons of test examples between the obtained EC-ANN model simulations and the Momentum simulations are presented in Fig. 8. Because of its symmetrical structure, $S(1,1)$ and $S(1,2)$ are chosen to characterize it. The good agreement between the two results confirm the validity of the proposed model for describing the electromagnetic behavior of various sized symmetrical cross junction discontinuities within these ranges.

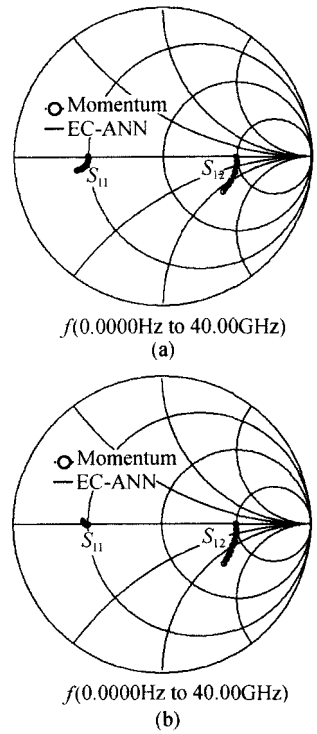

Fig. 8　Comparison EC-ANN for CPW symmetric cross junction　(a) $W = 70\mu m$, $G = 10\mu m$, $H = 30\mu m$; (b) $W = 50\mu m$, $G = 20\mu m$, $H = 50\mu m$

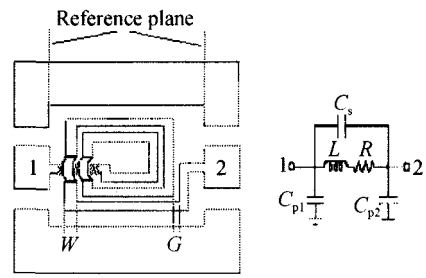

Fig. 9　CPW spiral inductor and its equivalent circuit

6　EC-ANN model for CPW spiral inductor

Lumped circuit elements such as spiral inductors have the potential to reduce the overall circuit size of MMIC balanced mixers[19] and other components. For example, a V-band (50.0 to 75.0 GHz) lumped 180° hybrid requires only 0.26 mm^2 of chip area, while a Lange coupler occupies about 3 mm^2 chip area, which is larger by a factor of 10[19].

A typical spiral inductor with two and half turns in the CPW environment and the lumped equivalent circuit model are shown in Fig. 9.

The inductance L and the parasitic capacitance C_{p1}, C_{p2}, and C_s in the model can be obtained using FDM[20], as well as from Z-parameters.

$$C_{p1} = -\frac{1}{\omega \mathrm{Im}\left(\frac{Z_{11}Z_{22} - Z_{12}Z_{21}}{Z_{22} - Z_{21}}\right)} \tag{10}$$

$$C_{p2} = -\frac{1}{\omega \mathrm{Im}\left(\frac{Z_{11}Z_{22} - Z_{12}Z_{21}}{Z_{12}}\right)} \tag{11}$$

$$Z = \frac{Z_{11}Z_{22} - Z_{12}Z_{21}}{Z_{12}} \tag{12}$$

$$L = \frac{1}{\omega} \times \sqrt{\frac{R(\mathrm{Re}(Z)^2 + \mathrm{Im}(Z)^2) - \mathrm{Re}(Z)R^2}{\mathrm{Re}(Z)}} \tag{13}$$

$$C_s = \frac{\mathrm{Re}(Z) - R}{\omega^2 \times \mathrm{Re}(Z) L + \omega R \times \mathrm{Im}(Z)} \quad (14)$$

The resistance R in the equivalent circuit is given by Ref. [20].

$$R = \begin{cases} R_{dc} + \{[R(1\,\mathrm{GHz}) \sqrt{f_g}] - R_{dc}\} \times \frac{f}{f_g}, & f < f_g \\ R(1\,\mathrm{GHz}) \sqrt{f}, & f > f_g \end{cases} \quad (15)$$

where the resistance is in ohms, frequency is in GHz, and

$$f_g = 39.131 \times \frac{\rho/\rho_{Cu}}{t}\ \mathrm{GHz} \quad (16)$$

The input parameters of the CPW spiral inductor EC-ANN model include line width W, gap width G and number of turns N, whose range are given in Table 7. Other physical parameters under consideration are fixed in this case. The output parameters are L, C_s, C_{p1}, and C_{p2}. There are 60 structures (examples) on which momentum simulations are performed over 0～40 Gz. Final ANN training data are given in Table 8.

Table 7 Variable parameter ranges for CPW spiral inductor

Parameter	Min	Max
W/μm	5	20
G/μm	5	15
N	1	6

Table 8 ANN training data of CPW spiral inductor

Training algorithm	Levenberg-Marquardt
Activation function	Tansig()
Training error	5.7×10^{-5}
Neurone of the input layer	3
Neurone of the output layer	4
Neurone of the hidden layer	20

In Fig. 10, test examples of the obtained EC-ANN models simulations and the Momentum simulations are compared. Again, the agreement between this model and the Momentum simulation can be seen and confirms the validity of the proposed model to describe the discontinuity electromagnetic behavior.

7 CPW filter-design example

The circuit-design example based on the CPW EC-ANN model, installed in an Agilent-ADS2003A, is a lumped element band pass filter on GaAs. The circuit schematic and micrograph are shown in Figs. 11 and 12, respectively.

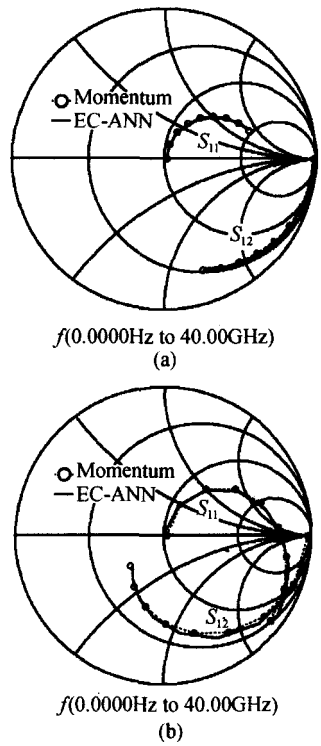

Fig. 10 Comparison EC-ANN for CPW spiral inductor (a) $W = 10\,\mu m$, $G = 10\,\mu m$, $N = 1.5$; (b) $W = 20\,\mu m$, $G = 10\,\mu m$, $N = 2.5$

The CPW EC-ANN models used in this design are step line ($W_1 = 70\,\mu m$, $W_2 = 100\,\mu m$, $T = 10\,\mu m$, $G = 10\,\mu m$), symmetric cross junction ($W = 70\,\mu m$, $G = 10\,\mu m$, $H = 30\,\mu m$, $n = 1$), interdigital capacitor (1 - $N = 1$, $n = 2.5$, $G = 10\,\mu m$, $T = 50\,\mu m$/2 - $N = 1$, $n = 3.5$, $G = 10\,\mu m$, $T = 105\,\mu m$), and spiral inductor ($W = 10\,\mu m$, $G = 10\,\mu m$, $N = 1.5$).

The filter has been designed for a center frequency of 20 GHz. Results are shown in Fig. 13 for circuit simulation by EC-ANN models and measured responses. Good agreement has been obtained

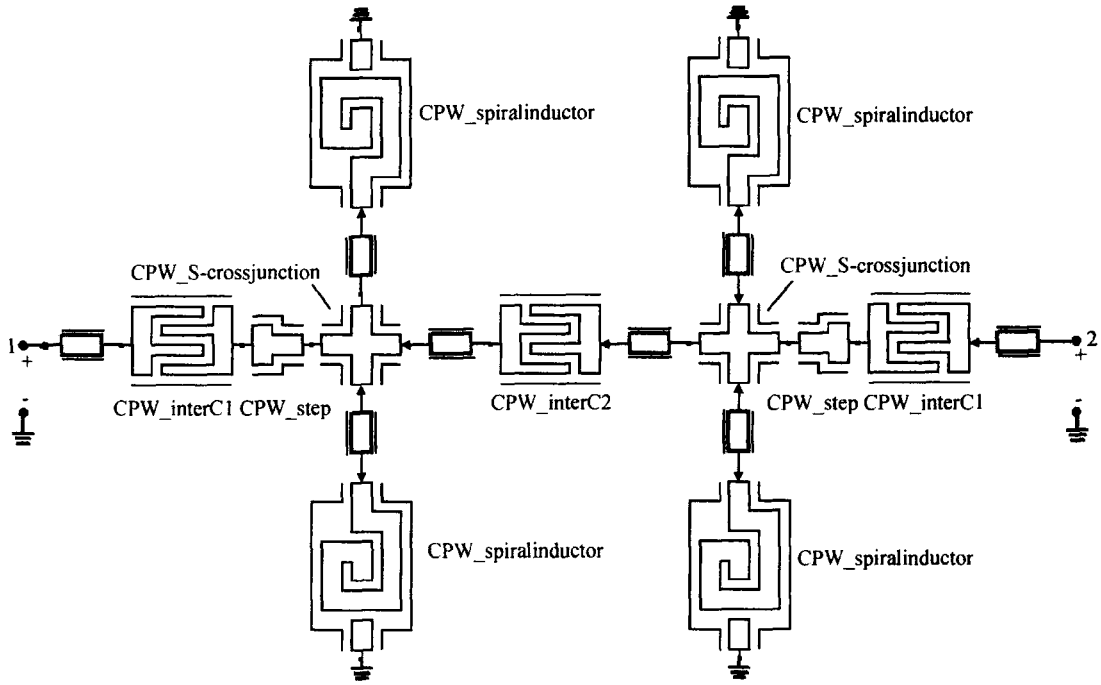

Fig. 11　Schematic of CPW lumped element band pass filter

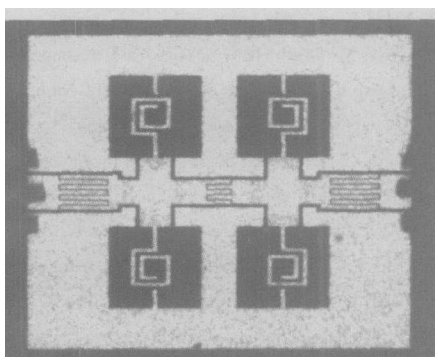

Fig. 12　Micrograph of CPW lumped element band pass filter

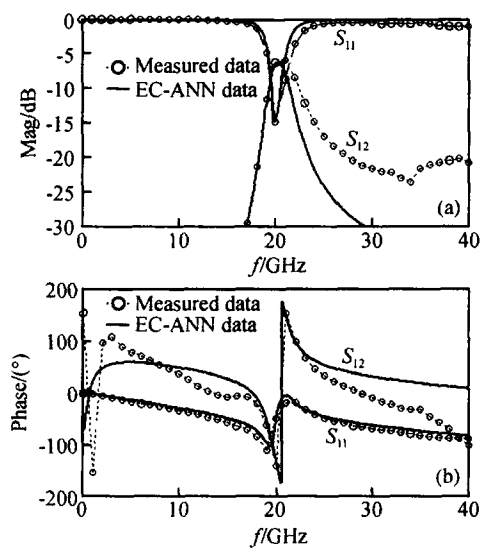

Fig. 13　CPW lumped element band pass filter response for the EC-ANN circuit simulation and real on-wafer measurement

between EC-ANN circuit design and measured results over the 0～40 GHz range. This demonstrates the application of EC-ANN models in CPW circuit design.

Using EC-ANN models for CPW components has allowed accurate and efficient design of the CPW filter. The amount of time required to provide EM simulation results for 40 frequency points for the entire filter circuit was approximately 25h on a PC (P4 processor/1G memory), while the circuit simulation time of the EC-ANN model under same condition is only 2.06s. This confirms substantial savings in computation time when these components are to be used over and over in different circuit designs.

It should be mentioned that even larger and more complex circuits can be designed using the developed EC-ANN models. EM simulation of larger complex circuits is limited by the computer resources available, and in many cases is not practi-

cal. With EC-ANN component modeling, these difficulties are overcome.

8 Conclusion

The results presented in this paper clearly demonstrate the application of the EC-ANN modeling approach for developing efficient and accurate models for various CPW components, and discontinuities. Models developed for CPW steps, symmetrical cross-junctions, interdigital capacitors, and spiral inductors can be conveniently used for efficient and accurate design of CPW circuits. The example of circuit design reported in this paper and verification of final design by comparing with measured results validates the modeling and design approach developed.

The methodology of EC-ANN modeling is applicable to other classes of microwave and millimeter-wave circuits, for which accurate component models are not yet available. Thus, we can look forward to increasing applications of the EC-ANN modeling approach in microwave and millimeter-wave design.

References

[1] Simons R N. Coplanar waveguide circuits, component, and system. Cleveland, Ohio, 2001

[2] Naghed M, Wolff I. Equivalent capacitance of coplanar waveguide discontinuities and interdigitated capacitors using a three-dimensional finite difference method. IEEE Trans Microw Theory Tech, 1990, 38: 1808

[3] Tran A, Itoh T. Full-wave modeling of coplanar waveguide discontinuities with finite conductor thickness. IEEE Trans Microw Theory Tech, 1993, 41: 1611

[4] Jin H, Vahldieck R. Full-wave analysis of coplanar waveguide discontinuities using the frequency domain TLM method. IEEE Trans Microw Theory Tech, 1993, 41: 1538

[5] Naghed M, Rittweger M, Wolff I. A new method for the calculation of equivalent inductance of coplanar waveguide discontinuities. IEEE MTT-S Int Microwave Sym Dig, Boston, MA, 1991: 747

[6] Mirshekar-Syahkal D. Computation of equivalent circuits of CPW discontinuities using quasi-static spectral domain method. IEEE Trans Microw Theory Tech, 1996, 44: 979

[7] Becks T, Wolff I. Full-wave analysis of various CPW bends and T-junctions with respect to different types of air-bridges. IEEE MTT-S Int Microwave Sym Dig, Atlanta, Ga, 1993: 823

[8] Heinrich W. Quasi-TEM description of MMIC coplanar lines including conductor-loss effects. IEEE Trans Microw Theory Tech, 1993, 41: 45

[9] Getsinger W J. End-effects in Quasi-TEM transmission lines. IEEE Trans Microw Theory Tech, 1993, 41: 666

[10] Mao M H, Wu R B, Chen C H, et al. Characterization of coplanar waveguide open end capacitance ——theory and experiment. IEEE Trans Microw Theory Tech, 1994, 42: 1016

[11] Beilenholf K, Klingbeil H, Heinrich W, et al. Open and short circuits in coplanar MMIC's. IEEE Trans Microw Theory Tech, 1993, 41: 1534

[12] Devabhaktuni V K, Yagoub M, Fang Y, et al. Neural networks for microwave modeling: Model development issues and nonlinear modeling techniques. Int J RF Microw Comput-Aided Eng, 2001, 11: 4

[13] Watson P M, Gupta K C. Design and optimization of CPW circuits using EM-ANN models for CPW components. IEEE Trans Microw Theory Tech, 1997, 45: 2515

[14] Khireddine S, Drissi M, Soares R. Neuronal approach for an accurate model of coplanar structures. EMC Compo, 2002

[15] Zhang Q J, Gupta K C, Devabhaktuni V K. Artificial neural networks for RF and microwave design-from theory to practice. IEEE Trans Microw Theory Tech, 2003, 51: 1339

[16] Liao Y. The application of artificial neural networks in microwave device modeling technology. Master Thesis, Hangzhou Institute of Electronics Engineering, Hangzhou, 2003

[17] Zhang Q J, Gupta K C. Neural networks for RF and microwave design. Norwood, MA: Artech House, 2000

[18] Montgomery D C. Design and analysis of experiment. New York: Wiley, 1991

[19] Pogatzki P, Kother D, Kulke R, et al. Coplanar hybrids based on an enhanced inductor model for mixer applications up to MM-wave frequencies. Proc 24th European Microwave Conf Dig, Cannes, France, 1994, 1: 254

[20] Abdo-Tuko M, Naghed M, Wolff I. Novel 18/36 GHz (M) MIC GaAs FET frequency doulbers in CPW-techniques under the consideration of the effects of coplanar discontinuities. IEEE Trans Microw Theory Tech, 1993, 41(8): 1307

共面波导不连续结构 EC-ANN 模型的电路设计与实现 *

胡　江[1]　孙玲玲[2]

(1 浙江大学信息与电子工程学系，杭州　310027)
(2 杭州电子科技大学微电子 CAD 研究所，杭州　310018)

摘要：将一种精确高效的等效电路训练人工神经网络模型引入共面波导不连续性结构建模.该建模算法继承了等效电路模型和电磁仿真人工神经网络模型的优点.此次开发并得到验证的共面波导不连续性结构模型包括:台阶段、叉指电容、对称十字节和螺旋电感.这些模型嵌入 CAD 仿真工具可以完成电路的设计、仿真和优化,最后通过一个 GaAs 工艺的共面波导带通滤波器的设计与实现验证了模型的有效性.

关键词：共面波导；不连续性结构；模型；等效电路；人工神经网络；带通滤波器
EEACC：2570A
中图分类号：TN43　　**文献标识码**：A　　**文章编号**：0253-4177(2005)12-2320-10

*国家自然科学基金(批准号:90207007)和浙江省重大合作计划(批准号:2004C14004)资助项目
2005-07-09 收到